PLENARY REPORT

THE VALIDITY OF QED AND HADRON PRODUCTION IN ELECTRON-POSITRON INTERACTIONS*

Roy F. Schwitters
Stanford Linear Accelerator Center
Stanford University, Stanford, California 94305, USA

ABSTRACT

Recent experimental tests of QED in high energy e^+e^- collisions, scans for narrow resonances, recent results in hadron production below 1.4 GeV center-of-mass energy, general properties of hadron production in the center-of-mass energy range 2.5 GeV to 7.4 GeV, and new results in the 4 GeV center-of-mass energy region are reviewed.

INTRODUCTION

Much has been learned from the study of high energy e^+e^- interactions during the two years since the London conference.[1] In this report, a small part of that work is reviewed; Björn Wiik will review other aspects of this rapidly growing field. Five topics to be covered here are: the current status of high energy tests of quantum electrodynamics in e^+e^- reactions, a summary of scans for narrow resonances, recent results on hadron production at center-of-mass energies $E_{c.m.}$ below 1.4 GeV, general properties of hadron production for $E_{c.m.}$ between 2.5 GeV and 7.4 GeV, and recent results on hadron production in the 4 GeV region of $E_{c.m.}$

I. HIGH ENERGY TESTS OF QED

At present, there are no known discrepancies between experiment and the theoretical predictions of QED that would invalidate the basic assumptions of the theory. Indeed, QED is the most successful theory in physics. High precision tests of QED were the subject of the invited paper of de Rafael[2] presented at this conference and will not be discussed here.

The short distance behavior of the theory may be tested[3] in e^+e^- interactions because of the very large values of q^2, the 4-momentum transfer squared, that is available with high energy e^+e^- storage rings. Generally, these tests of QED involve the measurement of two processes differing from one another by either the types of particles involved, the range of kinematic variables covered, or both. Often, one of the reactions is measured at small values of q^2; this is termed the luminosity monitor. The test reaction occurs with large values of q^2. The confrontation between experiment and theory is then the comparison of the relative yield observed for the two reactions to that expected from QED, where the appropriate theoretical cross sections are folded with detector acceptances. This is usually expressed as the ratio "EXP/QED" which is the ratio of the relative yield of the two reactions to the relative QED cross sections corrected for acceptances.

Since the QED cross sections of interest fall like powers of $1/q^2$, a low q^2 reaction will have high counting rates and experimental uncertainties in the luminosity monitor often are dominated by systematic errors in acceptance. Conversely, the test reaction usually will have relatively low counting rates and correspondingly large statistical errors.

In a paper submitted to this conference,[4] a Stanford-Penn group has reported new results on Bhabha scattering ($e^+e^- \to e^+e^-$) and two-quantum annihilation ($e^+e^- \to \gamma\gamma$) at $E_{c.m.}$ near 7 GeV. Both reactions were studied in the same apparatus at SPEAR. Similar studies at lower $E_{c.m.}$ have been published[5] by this group. The luminosity monitoring reaction was Bhabha scattering at angles near 4 degrees; the authors claim their systematic errors in this monitor are less than 0.5%. Note that this demands that the errors in determining the scattering angle be less than 0.1 mr. Test reactions were observed in two nonmagnetic spectrometers composed of tracking chambers and large NaI absorption counters which were oriented perpendicular to the incident beam direction. The theoretical cross sections with radiative corrections to order α^3 were computed using the methods of Berends, Gaemers, and Gastmans.[6] The results, presented in Table I, are in excellent agreement with QED.

TABLE I

Summary of results on Bhabha scattering ($e^+e^- \to e^+e^-$) and two-quantum annihilation ($e^+e^- \to \gamma\gamma$) from the Stanford-Pennsylvania experiment.[4]

$E_{c.m.}$ (GeV)	7.0	7.4
Bhabha events observed	1118	1241
Bhabha events expected	1067	1300
EXP/QED for Bhabha scattering	1.05 ± 0.04	0.96 ± 0.03
$\gamma\gamma$ events observed	177	297
$\gamma\gamma$ events expected	163	333
EXP/QED for two-quantum annihilation	1.08 ± 0.09	0.89 ± 0.07

It is customary to use such results to set limits on breakdown parameters $\Lambda_\pm$ which are a way to describe deviations from QED arising through modification of propagators in lowest order Feynman diagrams.[3] Bhabha scattering tests the photon propagator which is modified by:

$$1/q^2 \to (1/q^2)\,[1 \pm q^2/(q^2 - \Lambda_\pm^2)]\,. \qquad (1)$$

Two-quantum annihilation is sensitive to modifications of the electron propagator that can be parametrized by

$$\frac{1}{q^2 - m^2} \to \frac{1}{q^2 - m^2}\,(1 \pm q^4/\Lambda_\pm^4) \qquad (2)$$

m is the electron mass and $\Lambda_\pm$ are the breakdown parameters. Lower limits for $\Lambda_\pm$ obtained from the Stanford-Pennsylvania experiment are presented in Table II. Notice that the limits for $\Lambda_\pm$ are rather insensitive to experimental errors, but depend strongly on $E_{c.m.}$ For example, if the systematic uncertainty in luminosity monitoring for this experiment is really ±5%, the various limits on $\Lambda_\pm$ in Table II decrease by 5% to 20%. These limits are comparable to or greater than those set in an earlier experiment[7] by the SLAC/LBL group using the magnetic detector at SPEAR and indicate that QED is valid to scales of distance as small as 10^{-15} cm.

TABLE II

Limits on possible breakdown parameters $\Lambda_\pm$ determined by Ref. 4.

Reaction	Lower limits (95% confidence level) Λ_+ (GeV)	Λ_- (GeV)
$e^+e^- \to e^+e^-$	38.0	33.3
$e^+e^- \to \gamma\gamma$	10.9	8.9

There are now several examples where the simple predictions of QED do not describe experimental results. These occur at $E_{c.m.}$ corresponding to vector meson masses and are not interpreted as a breakdown of QED, but as an interference between the resonance production amplitude for some electrodynamic final state and the normal QED amplitude. This interference effect was first observed at ACO[8] through the reaction $e^+e^- \to \mu^+\mu^-$ in the vicinity of the ϕ meson. The most dramatic demonstrations of this effect have been seen within the last two years at energies corresponding to the very narrow resonances ψ and ψ'. Interference data from the SLAC/LBL group[9] are presented in Fig. 1. The radical departures of these data from the simple predictions of QED are in complete agreement with the expected interference between a narrow resonance and QED.

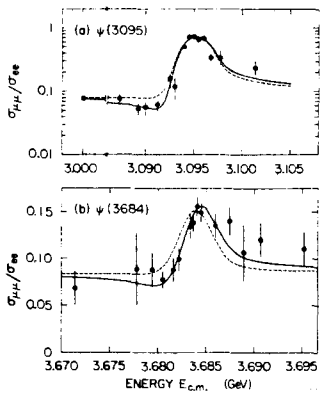

Fig. 1--Ratio of muon pair production to Bhabha scattering in the vicinity of the ψ (a) and ψ' (b) resonances. The solid curves are the expected interference patterns.

In summary, QED well describes all 2-body electrodynamic processes measured to date in high energy e^+e^- collisions when appropriate hadronic and radiative corrections are applied to the theory. The future for QED experiments with the new machines PEP and PETRA looks very bright because we may be able to measure weak-electrodynamic interference effects, rather than only to set limits on modifications of QED. The rapporteur at the XXI International Conference on High Energy Physics should have some very interesting things to say on this subject.

II. HADRON PRODUCTION - SEARCHES FOR NARROW RESONANCES

With the discovery of the very narrow resonances ψ and ψ', several groups at various laboratories initiated searches for additional narrow resonances in the $J^{PC} = 1^{--}$ channel by measuring the total hadronic cross section σ_T in very fine steps in $E_{c.m.}$ (usually 2 MeV increments). Since the step sizes were chosen to be comparable to the energy spread of the beams, even resonances very narrow compared to the energy resolution will show up as peaks over a few bins in $E_{c.m.}$ and the area under their production cross sections can be measured. This area is related to the partial decay width of the resonance (J = 1 assumed) to electron pairs Γ_{ee} by

$$Bh\,\Gamma_{ee} = \frac{2\alpha^2}{9\pi} \int_{\text{resonance}} R\,dE_{c.m.} \qquad (3)$$

where $R \equiv \sigma_T/\sigma_{\mu\mu}$, $\sigma_{\mu\mu}$ (= 86.8 nb/$E^2_{c.m.}$ (GeV)) is the pointlike muon pair cross section. Bh is the branching ratio of the resonance to hadrons and is usually assumed to be close to one.

Fine scans for new resonances have now been reported from Novosibirsk, Frascati, and SPEAR; a summary of these measurements and the approximate upper limits which can be set for Γ_{ee} are given in Table III. In most cases, the

TABLE III

Summary of searches for narrow vector states

Mass Range (GeV)	Approx. 90% confidence level upper limit on Γ_{ee} (eV)	Group (Ref.)
0.78 - 1.34	100	Novosibirsk (10)
1.9 - 2.5	500	Frascati - $\gamma\gamma$ (11)
2.9 - 3.1		- MEA (12)
2.5 - 3.0	500	Frascati (13)
3.2 - 7.8	500	SLAC/LBL (14,15)
5.7 - 6.4	100	SLAC/LBL (16)
		Maryland, Princeton, Pavia, San Diego (17)
7.0 - 7.4	60	SLAC/LBL (16)

upper limits on Γ_{ee} are an order of magnitude smaller (or even less) than the Γ_{ee} of the known vector mesons, indicating that new narrow vector states are unlikely to exist in the mass ranges covered.

III. HADRON PRODUCTION BELOW 1.4 GeV

Important new results on hadron production with $E_{c.m.}$ below 1.4 GeV have been reported to this conference by groups from Novosibirsk[18] and Orsay.[19] Using a new detector and the VEPP-2M storage ring, the Novosibirsk group has been able to accumulate substantially more information on hadron production from the ϕ mass to 1.34 GeV than previously existed. In Fig. 2, cross sections are presented for the reactions $e^+e^- \to \pi^+\pi^-\pi^+\pi^-$ and $e^+e^- \to \pi^+\pi^-\pi^0\pi^0$. These new Novosibirsk results are superior to the previous data in both the number of data points and their statistical accuracy. In both reactions, the cross section shows a smooth variation with $E_{c.m.}$ from threshold to nearly 1.4 GeV. There is no evidence for any structure in either reaction. Previously,[20] it was conjectured that a $\rho'(1250)$ could be contributing to possible structure in the $\pi^+\pi^-\pi^0\pi^0$ channel. The present results would argue against such a state and seem to show the simple threshold behavior expected for phase space production of the 4-pion channel. The smooth curve in Fig. 2a shows the threshold behavior expected for 4 pions produced in the state $\rho^0\pi^+\pi^-$ where the ρ and pions are in relative s-waves. The smooth curve in Fig. 2b includes one-half the $\rho^0\pi^+\pi^-$ cross section determined from the $\pi^+\pi^-\pi^+\pi^-$ fit and an additional contribution from $\omega^0\pi^0$ production. The data are well described by these simple threshold models and do not indicate the presence of any new resonances in this region of $E_{c.m.}$.

It is interesting to note that the total 4-pion cross section near $E_{c.m.}$ = 1.3 GeV is very nearly equal to the muon pair production cross section at this energy. As discussed below, the total hadronic cross section "scales" in the $E_{c.m.}$ range 2.5 GeV to 4 GeV with a value approximately 2.5 times the muon pair cross section. Thus, we can already account for roughly one-half of this scaling cross section at $E_{c.m.}$ = 1.3 GeV.

The reaction $e^+e^- \to \pi^+\pi^-$ has been recently studied by groups at Orsay[19,21] and Novosibirsk.[18] These experiments yield information on the pion form factor F_π for timelike values of q^2. F_π is related to the $\pi^+\pi^-$ cross section by:

$$\frac{d\sigma}{d\Omega} = \frac{\alpha^2}{8E^2_{c.m.}}\beta^3\sin^2\theta\,|F_\pi(E^2_{c.m.})|^2 \qquad (4)$$

where α is the fine structure constant, β is velocity of the pion, and the production angle θ is measured with respect to the incident e^+ direction.

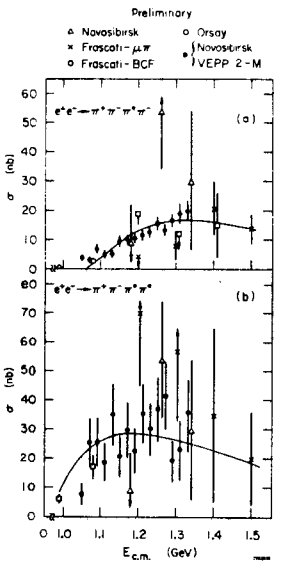

Fig. 2--Total cross sections for the reactions (a) $e^+e^- \to \pi^+\pi^-\pi^+\pi^-$ and (b) $e^+e^- \to \pi^+\pi^-\pi^0\pi^0$. The solid points are the new data from Novosibirsk presented to this conference by Sidorov.[16] The solid curves are threshold model fits to the data computed by the Novosibirsk group.

Our present knowledge of $|F_\pi|^2$ is summarized in Figs. 3 and 4. The Orsay magnetic detector[21] has measured $|F_\pi|^2$ below the ρ peak and the results are in excellent agreement with the formula of Gounaris and Sakurai.[22] New results from Orsay[19] above 900 MeV indicated a systematic departure above the Gounaris-Sakurai formula. The new results from Novosibirsk shown in Fig. 4 confirm this excess of $\pi^+\pi^-$ production above 900 MeV. The two smooth curves in Fig. 4 are the ρ-tail extrapolated from the Gounaris-Sakurai formula and the result of the interference of a $\rho'(1250)$ with the ρ-tail. The data clearly prefer an additional contribution to $|F_\pi|^2$, but cannot be said to establish the existence of a $\rho'(1250)$. The excess of $\pi^+\pi^-$ production is likely to be simply related to the onset of 4-pion production which occurs at essentially the same energy, and not to resonance production. More experimental and theoretical work is needed to clarify this situation.

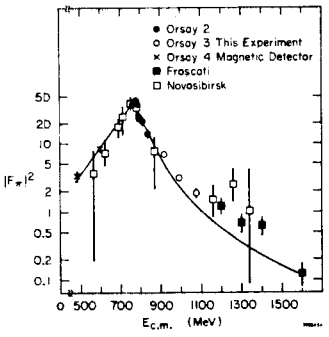

Fig. 3--The pion form factor vs $E_{c.m.}$ in the vicinity of the ρ meson. The data include published points from Novosibirsk and Orsay as well as recent data from Orsay.[19] The smooth curve is the Gounaris-Sakurai formula.

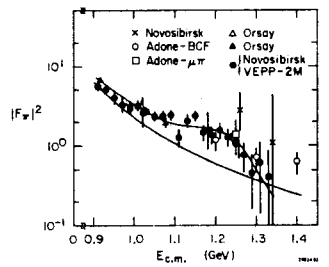

Fig. 4--The pion form factor above the ρ meson. The solid points are recent data from Novosibirsk[18] and Orsay.[19] The lower curve is the Gounaris-Sakurai formula. The upper curve shows the additional contribution possible from a $\rho'(1250)$.

The ϕ meson has been studied extensively in e^+e^- collisions and new results were reported to this Conference from Novosibirsk[18] and Orsay.[19] In connection with some very interesting work on transverse beam polarization (discussed in the invited talk of Skrinsky),[23] the Novosibirsk group produced the remarkable excitation curve for the ϕ shown in Fig. 5. They were able to measure the g-2 spin precession frequency of a stored beam in VEPP-2M and thereby accurately calibrate the machine energy and, therefore, the ϕ mass. Their value is:

$$m\phi = 1019.48 \pm 0.13\ \text{MeV}/c^2 \qquad (5)$$

The same group obtained a comparable result by determining the range of charged K mesons produced at the ϕ peak.

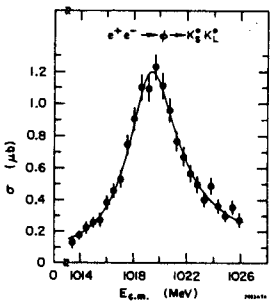

Fig. 5--Excitation curve for the ϕ meson obtained with the VEPP-2M storage ring.[18]

The $\pi^+\pi^-\pi^0$ final state has been studied at values of $E_{c.m.}$ away from the ω and ϕ masses in order to detect the interference of the ω and ϕ amplitudes. As first reported by the Orsay group,[21] there exists an interference in this channel with the relative phase between the ω and ϕ amplitudes approximately equal to 180 degrees. This result is confirmed by the large sample of data presented to this Conference by the Novosibirsk group.[18] Finally, the Orsay group[19] has studied the Dalitz plot for the decay $\phi \to \pi^+\pi^-\pi^0$ and concludes that greater than 80% of these decays proceed through the quasi-2-body decay $\phi \to \rho\pi$.

In summary, hadron production below 1.34 GeV is dominated by the well-known resonances ρ, ω, ϕ with interferences between these resonances occurring in several channels. The production of four pions exhibits a simple threshold behavior with no evidence for a $\rho'(1250)$ resonance. At 1.3 GeV, the 4-pion cross section is approximately equal to the muon pair cross section. There exists an excess of $\pi^+\pi^-$ production over that expected from the Gounaris-Sakurai formula for the ρ-tail at $E_{c.m.} \gtrsim 900$ MeV. While this excess may be due to a proposed $\rho'(1250)$ resonance, the data probably can be explained by inelastic effects arising from the opening of the 4-pion channel at nearly the same energy.

IV. GENERAL PROPERTIES OF HADRON PRODUCTION BETWEEN 2.5 GeV AND 7.4 GeV

The general properties of multihadronic final states in e^+e^- annihilation have been discussed in detail at a number of conferences[15,24] and will be reviewed only briefly in this report. Through what must rank as one of the major achievements in high energy physics over the past two years we now have a vast body of experimental information on hadron production that can be described in general terms by the quark-parton model where hadrons are produced through the point-like coupling of spin-$\frac{1}{2}$ partons to the electromagnetic current.

One of the most important experimental quantities in the study of multihadron production is the ratio R of the total hadronic cross section to the point-like cross section for producing muon pairs. In quark models, at sufficiently high energies, R is related to the quark charges by:

$$R = \sum_{s=\frac{1}{2}} Q_i^2 + \tfrac{1}{4} \sum_{s=0} Q_i^2 \qquad (6)$$

where the two summations are over spin-$\frac{1}{2}$ and spin-0 quarks. The Q_i are the quark charges in units of the electron charge. Fig. 6 summarizes our present experimental understanding of R from $E_{c.m.} \approx 2$ GeV to $E_{c.m.} \approx 8$ GeV. New results on R in the $E_{c.m.}$ range 2-3 GeV were presented to this Conference by the $\gamma\gamma$ group at Frascati;[13] the previous SLAC/LBL results[15,25] are also presented in Fig. 6.

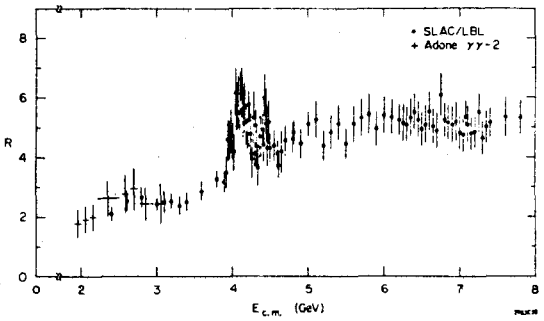

Fig. 6--The ratio R of the total hadronic cross section to the muon pair cross section. Radiative tails from the ψ and ψ' resonances have been removed.

Over this energy range, R has three distinct regions aside from the ψ and ψ' resonances: $E_{c.m.} \lesssim 3.8$ GeV where $R \approx 2.5$, $E_{c.m.} \gtrsim 5$ GeV where $R \approx 5.5$, and the 4 GeV region where R exhibits a very complicated transition zone. A constant value of R is termed "scaling" and is expected in quark-proton models as discussed above. The low energy region where $R \approx 2.5$ is in reasonable agreement with the predictions of quark models having three flavors of ordinary quarks in three colors where R is expected to be 2. The transition region of R near 4 GeV strongly suggests that new hadronic degrees of freedom are being excited here. This region will be discussed in Section V. The value of R above 5 GeV is too large to be satisfactorily accounted for by only the excitation of charmed particles (where $R = 3\frac{1}{3}$) and may indicate the presence of additional quarks beyond charm, a heavy lepton,[26] or both.

Presently available data on the mean charged multiplicity in multihadron production are given in Fig. 7. Within the rather large errors, all the data are consistent with a logarithmic energy dependence similar to that observed in hadron production by hadron beams at comparable c.m. energies.[28]

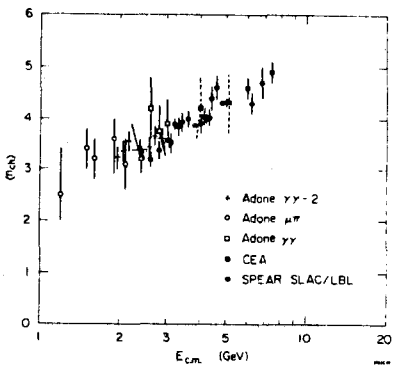

Fig. 7--Mean charged multiplicity in hadron events produced by e^+e^- annihilation. Adone $\gamma\gamma$-2 results are new;[13] a list of previous references may be found in Ref. 27.

An interesting inclusive property of hadron production that has been known for some time now[1] is the observation by the SLAC/LBL group that the fraction of $E_{c.m.}$ appearing in charged particles decreases from 0.6 near $E_{c.m.} = 2.5$ GeV to less than 0.5 at $E_{c.m.} = 7.4$ GeV, as shown in Fig. 8. Naively, one expects this fraction to be 0.67, but the production of particles other than pions could reduce it somewhat. Why it decreases with increasing $E_{c.m.}$ is not understood, however. Presumably, this is related to the production of new particles in the 4 GeV region. However, as pointed out Azimov, Frankfurt and Khoze,[29] it cannot be due entirely to a heavy lepton production because the data used only three or more charged prong events while heavy leptons are expected to contribute primarily to events with only two charged prongs.

Single particle inclusive spectra for hadrons produced in e^+e^- annihilation can be described by the following simple formula[30]

$$\frac{d\sigma}{d\Omega dx} = \frac{\alpha^2}{s} \beta x \, F(x, E_{c.m.}) \left[1 + a(x, E_{c.m.}) (\cos^2\theta + P^2 \sin^2\theta \cos 2\phi) \right] \qquad (7)$$

where $x = 2E_h/E_{c.m.}$, E_h is the hadron energy, β is its velocity, θ, ϕ are the polar and azimuthal angles of the produced hadron measured from the e^+ direction and horizontal plane, $s = E_{c.m.}^2$, and P is the transverse (vertical) single beam polarization. In general, F and a are functions of x and $E_{c.m.}$ (or E_h); should F and a depend only on x, the cross section is said to scale and the quantity $sd\sigma/dx$ should depend only on x.

In Fig. 9, $sd\sigma/dx$ (measured by the SLAC/LBL collaboration[15]) is plotted versus x. In these measurements the hadron momentum rather than total energy was used to compute x because momenta are the directly measured quantities. At low values of x, $sd\sigma/dx$ depends strongly on $E_{c.m.}$, while for $x \gtrsim 0.4$, $sd\sigma/dx$ does not vary significantly with $E_{c.m.}$. Thus scaling obtains for $x \gtrsim 0.4$ from $E_{c.m.} = 3$ GeV to 7.4 GeV. A more critical study of scaling is provided by Fig. 10, where $sd\sigma/dx$ is plotted vs $E_{c.m.}$ for several bands of x. Aside from the lowest x band, there is little variation with $E_{c.m.}$ for $x \gtrsim 0.4$ except in the vicinity of $E_{c.m.} \approx 4$ GeV, where there seems to be a slight excess at intermediate values of x. Above 4 GeV, scaling holds for $x \gtrsim 0.2$ to about the 20% level, which is consistent with probable systematic errors of this experiment.

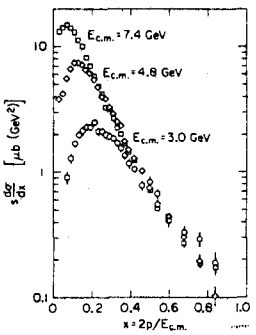

Fig. 9--$sd\sigma/dx$ vs x for three values of $E_{c.m.}$.

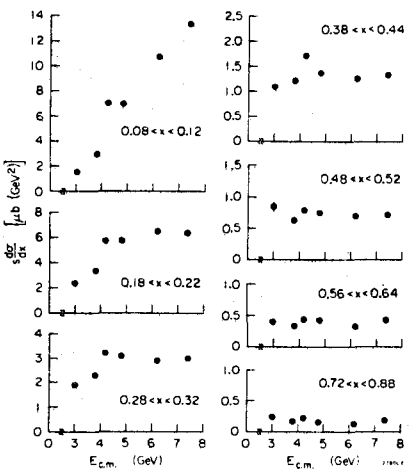

Fig. 10--$sd\sigma/dx$ vs $E_{c.m.}$ for various bands of x.

The scaling of $sd\sigma/dx$ is expected in the parton model,[31] where hadron production by e^+e^- annihilation is viewed as the production of pairs of partons followed by the subsequent decay of the partons into "jets" of hadrons. The slow multiplicity growth arises naturally in this picture as the mechanism to fill the central region in rapidity between the two jets. This picture is consistent with the observation by the SLAC/LBL group[32,24] of multiparticle correlations in hadronic events that have the appearance of back-to-back jets of hadrons.

In the SLAC/LBL analysis, a jet is defined as a multiparticle correlation that leads to a preferred direction in a hadronic event about which the momenta perpendicular to that direction are limited to values smaller than those expected

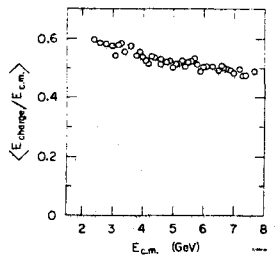

Fig. 8--Mean fraction of visible energy in charged prongs to $E_{c.m.}$. Data are from the SLAC/LBL group.[15]

from phase space considerations alone. To search for jets, hadronic events with three or more charged prongs are selected and the axis which minimizes the sum of squares of charged particle momenta perpendicular to it is found. This axis is called the jet axis for the event. A quantity called the sphericity (defined to be proportional to the sum of squares of momenta perpendicular to the jet axis divided by the sum of squares of the total momenta) is computed for each event. Small sphericity corresponds to very "jet-like" events. Sphericity distributions at three values of $E_{c.m.}$ are shown in Fig. 11 along with the distributions calculated from a Lorentz invariant phase space model and a "jet" model of hadron production. In the jet model, phase space is modified by a matrix element squared of the form:

$$|M|^2 \propto e^{-\left(\sum_i p_{\perp i}^2\right)/r^2} \qquad (8)$$

where $p_{\perp i}$ is the momentum of the i-th particle relative to the jet axis and r is an adjustable parameter.

As can be seen in Fig. 11, the data are well described by the jet model at all values of $E_{c.m.}$ while they systematically deviate from the phase space model as $E_{c.m.}$ increases. Values for the parameter r that are preferred by the data give a mean $p_\perp$ of approximately 300 MeV/c for all $E_{c.m.}$. A study[24,32] of effects arising from resonance production and more complicated phase space models failed to find any satisfactory description of the observed sphericity and inclusive momentum spectra, other than the jet model. Fig. 12 shows the comparison of the jet model and phase space model with the observed inclusive momentum spectrum at $E_{c.m.} = 7.4$ GeV. Again, the data prefer the jet model; the number of prongs with $x \gtrsim 0.5$ cannot easily be accounted for by phase space alone.

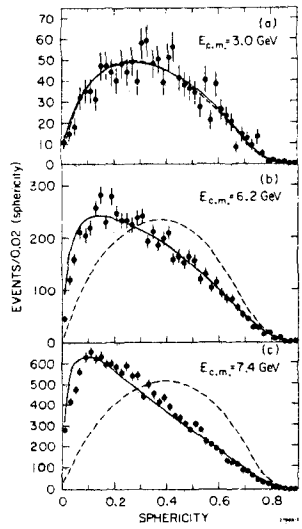

Fig. 11--Sphericity distributions for multihadron events, compared with Monte Carlo models of hadron production.

The distribution of hadrons relative to the jet axis is reminiscent of hadron distributions in hadron-hadron collisions measured relative to the incident beam direction. For example, Fig. 13 shows the distribution of hadrons in rapidity relative to the jet axis at three values of $E_{c.m.}$. We see the emergence of a plateau that grows in width, but not height, with increasing $E_{c.m.}$ in a manner very similar to hadron-hadron collisions. As mentioned previously, the mean value of momenta perpendicular to the jet axis is approximately 300 MeV/c.

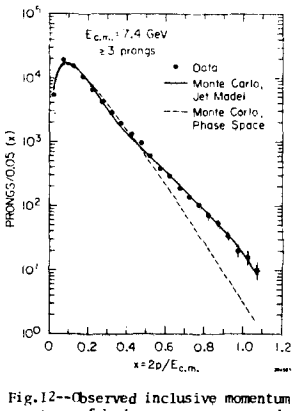

Fig. 12--Observed inclusive momentum spectrum of hadron prongs compared with Monte Carlo models.

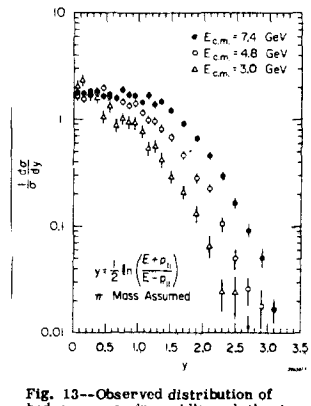

Fig. 13--Observed distribution of hadron prongs in rapidity relative to the jet axis.

The most dramatic difference between the jets observed in e^+e^- collisions and ordinary hadron collisions is in the angular distribution of the jet axis. In e^+e^- annihilation, the angular distribution must have the form of Eq.(7), while in ordinary hadron collisions the "jet" axis is the beam direction. The azimuthal distribution of the jet axis measured by the SLAC/LBL group at two values of $E_{c.m.}$ is shown in Fig.14. At $E_{c.m.}$=6.2 GeV, where the beam polarization P is very small, the distribution is flat; at $E_{c.m.}$=7.4 GeV,where P 80%, there is a strong cos 2ϕ term evident.

Corrected for acceptance losses, the data of Fig.14b indicate that the angular distribution of the originally produced jet axis is given by:

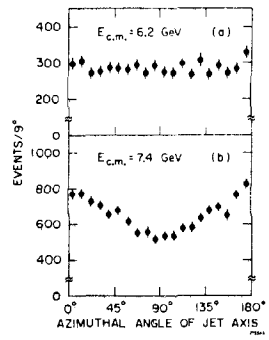

Fig. 14--Azimuthal distributions of the jet axis. At $E_{c.m.}$=7.4 GeV, the incident beams were transversely polarized.

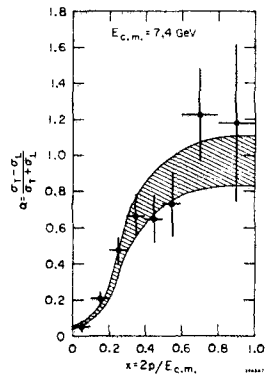

Fig. 15--a(x) (see Eq. (7)) vs x for charged tracks in multihadronic events. The shaded area is the jet model calculation.

$$\frac{d\sigma}{d\Omega}\text{jet} \propto 1+(0.97\pm0.14)(\cos^2\theta+P^2\sin^2\theta\cos 2\phi) \qquad (9)$$

This distribution is consistent with a = 1 for the jet, the largest value of a possible. In the context of the parton model, such a value of a suggests that the partons responsible for jets are spin-$\frac{1}{2}$ objects rather than, say, spin-0 where a would be -1.

The simple jet model that was used in the sphericity analysis is able to reproduce well the inclusive angular distribution of the produced hadrons when the jet axis has the angular distribution of Eq. (9). In Fig. 15, the function a(x) from Eq. (7) for multihadronic data taken at $E_{c.m.}$=7.4 GeV is plotted vs x. a(x) was determined[33] from a simultaneous fit to the θ and ϕ angular distributions; at this energy, the incident beams were transversely polarized. The same quantity calculated with the jet model lies within the shaded region of Fig. 15. Once again, the simple limited transverse momentum jet model represented by Eq. (8) is able to describe well an inclusive property of multihadronic events - in this case, the inclusive angular distribution.

In summary, some of the important general features of multihadron production between $E_{c.m.}$ = 2.5 GeV and $E_{c.m.} \approx$ 8 GeV are:

1. Aside from the very narrow resonances ψ and ψ', R scales in two regions of $E_{c.m.}$. For 2.5 GeV $\lesssim E_{c.m.} \lesssim$ 4 GeV, R ≈ 2.5, while for 5 GeV $\lesssim E_{c.m.} \lesssim$ 8 GeV, R ≈ 5. Present systematic errors on these values are approximately ±10% in overall normalization and a further ±10% smooth variation with $E_{c.m.}$ from lowest $E_{c.m.}$ to highest. A complicated transition region joins these two regions of R.
2. Within the experimental uncertainties of ±20%, the inclusive momentum spectra exhibit scaling for $x \gtrsim 0.4$ over all energies studied and for $x \gtrsim 0.2$ for $E_{c.m.} \gtrsim 5$ GeV.
3. The sphericity distribution of multihadronic events is peaked to lower values of sphericity than would be expected from phase space production alone, which implies that hadrons are produced in jets with $\langle p_\perp \rangle \approx$ 300 MeV for hadrons relative to the jet axis.
4. The inclusive angular distribution of hadrons at $E_{c.m.}$ = 7.4 GeV varies from isotropic for hadrons with $x \gtrsim 0.1$ to nearly $1+\cos^2\theta$ for prongs with $x \gtrsim 0.6$.
5. The mean charged multiplicity grows slowly with increasing $E_{c.m.}$, while the fraction of $E_{c.m.}$ appearing in charged particles decreases in a manner that cannot be explained by heavy lepton production.

Most of these features are remarkably well described by the quark-parton model with the partons having spin-$\frac{1}{2}$. A simple limited transverse momentum jet model is able to quantitatively reproduce the shapes of the sphericity, inclusive momentum, and inclusive angular distributions. This has not been possible in phase space or resonance production models proposed to date. The value of R below 4 GeV and the slow multiplicity growth are also features expected in the quark-parton model. The large value of R above 4 GeV is less easy to understand, however. The four quarks of the charm model are, by themselves, not able to account for this value of R. The detailed understanding of the magnitude of R in this energy region remains an outstanding question.

There is still other experimental information we would like to have. For example, studies of the correlation in quantum numbers between the two "halves" of jets will provide clues to their origins. The lepton component in multihadronic events awaits measurement. As the new higher energy machines become available, the most burning issue will again be the measurement of R. Does it increase, remain constant, or decrease?! If the simple scaling rules already observed in jets continue to apply at higher energies, the jets at PEP and PETRA

should be spectacular, indeed. If we are lucky, we will only have to wait until the XX International Conference to find out.

V. THE 4 GeV REGION

Hadron production near $E_{c.m.} = 4$ GeV exhibits a richness of structure that we are just beginning to extract. Our present knowledge of R in this region comes from preliminary results of the SLAC/LBL collaboration shown in Fig. 16. The main features are the possible broad peak near 3.95 GeV, the very

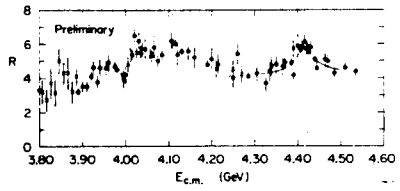

Fig. 16--R vs $E_{c.m.}$ in the 4 GeV region.

sharp rise from 4.00 GeV to 4.03 GeV, a second possible broad peak near 4.12 GeV, and the resonance-like structure[34] at 4.414 ± 0.007 GeV that has a width $\Gamma = 33 \pm 10$ MeV. The areas under all of these structures correspond to partial decay widths (see Eq. (3)) to electron pairs on the order of 10% of the ψ partial width. The rise in R and appearance of broad structures strongly suggest that the 4 GeV region represents the threshold for new particle production, at least some of which is likely related to the very narrow ψ and ψ' states. There have been many attempts to understand the structure in the 4 GeV region in terms of charmonium levels above charmed particle threshold[35] and collective "molecular" states of charmed particles,[36] but as yet there is no compelling and predictive theory of this structure.

The first direct observation of decays of new particles produced in this region has been reported recently by the SLAC/LBL group.[37] in a sample of 29,000 hadronic events collected between $E_{c.m.} = 3.90$ GeV and $E_{c.m.} = 4.60$ GeV, they observed 110 ± 24 decays of a new state to the final states $K^+\pi^-$ and $K^-\pi^+$. In the same sample of data, a signal of 124 ± 21 neutral combinations of the particles $K^\pm\pi^\mp\pi^+\pi^-$ was found at the same invariant mass. Both states appear to represent different decay modes of the same object; its mass is 1865 ± 15 MeV/c^2 and its decay width is less than 40 MeV/c^2.

The evidence for this state is presented in Fig. 17. In the top row of this

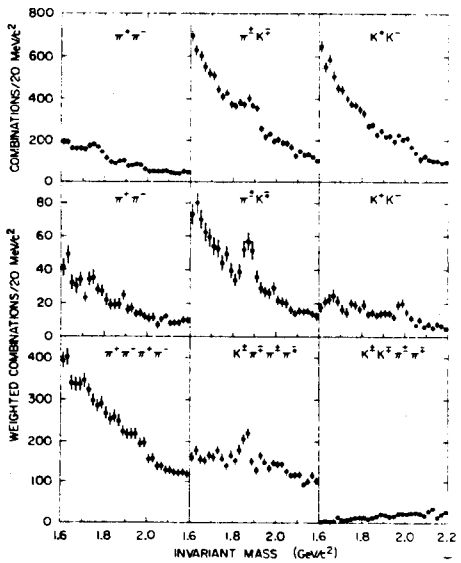

Fig. 17--Invariant mass spectra for neutral combinations of charged particles. (a) $\pi^+\pi^-$ assigning π mass to all tracks, (b) $K^\pm\pi^\mp$ assigning K and π masses to all tracks, (c) K^+K^- assigning K mass to all tracks, (d) $\pi^+\pi^-$ weighted by time-of-flight probability, (e) $K^\pm\pi^\mp$ weighted, (f) K^+K^- weighted, (g) $\pi^+\pi^-\pi^+\pi^-$ weighted by 4π time-of-flight probability, (h) $K^\pm\pi^\mp\pi^+\pi^-$ weighted by K3π probability, (i) $K^+K^-\pi^+\pi^-$ weighted by KK$\pi\pi$ probability.

figure, invariant mass spectra are plotted for all possible neutral combinations of two charged prongs assuming both pion and K masses for the prongs. Through kinematic reflections, a signal appears near 1.74 GeV/c in the $\pi\pi$ channel, 1.87 GeV/c^2 in the πK channel, and 1.98 GeV/c^2 in the KK channel. To establish the correct choice of final-state particles, time-of-flight information was used. Because the typical time difference between a K and a π in the signal region was comparable to the measurement resolution, the two particle combinations were weighted by their relative $\pi\pi$, πK, and KK likelihoods to extract maximal information on particle identity. Invariant mass spectra weighted in this manner are presented in the second row of Fig. 17. The Kπ hypothesis for the peak near 1.87 GeV/c^2 is clearly preferred over either $\pi\pi$ or KK; the residual peaks in the $\pi\pi$ and KK channels are consistent with the known time-of-flight resolution. The third row of Fig. 17 shows similarly weighted spectra for neutral combinations of four charged particles. Here, the K-π time-of-flight separation is greater and the only significant peak is in the K3π channel near 1.86 GeV/c^2.

The recoil mass spectra associated with these peaks, Fig. 18, and the lack of a signal in the large body of data at the ψ' mass indicate that this new state is produced with a threshold near 4 GeV in association with particles of comparable or even greater mass.

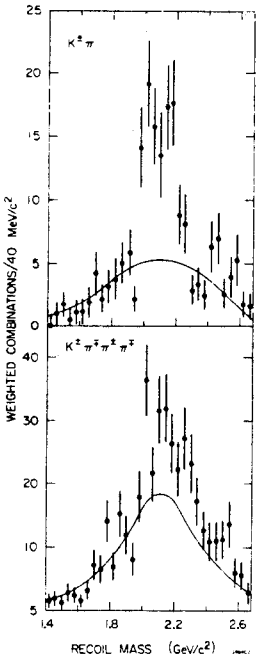

Fig. 18--Recoil mass spectra for combinations in the Kπ and K3π peaks. Smooth curves are estimates of the background obtained from combinations whose masses are on either side of the peak mass region.

To further study this new state and to search for others, the SLAC/LBL group[38] subsequently collected 19,000 hadronic events at the fixed $E_{c.m.} = 4.03$ GeV and present preliminary results from the new data at this Conference. $E_{c.m.} = 4.03$ GeV was chosen because it corresponds to the top of the very sharp rise in R mentioned previously. In a preliminary analysis, shown in Fig. 19, the Kπ signal at 1.87 GeV/c^2 stands out in the new data as an unmistakable feature above a small background. The recoil mass spectrum for events within this peak is presented in Fig. 20. The most prominent features are two large peaks above a smooth

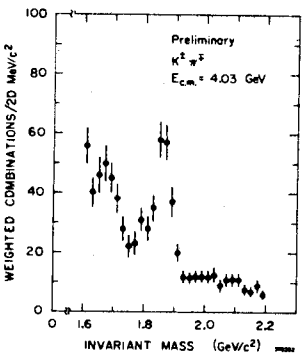

Fig. 19--Preliminary $K^\pm\pi^\mp$ invariant mass spectrum at $E_{c.m.} = 4.03$ GeV, weighted by time-of-flight probability.

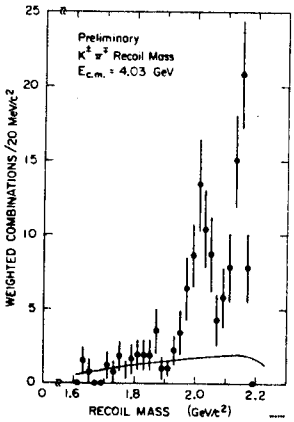

Fig. 20--Recoil mass spectrum for Kπ events in the 1.87 GeV/c^2 peak at $E_{c.m.} = 4.03$ GeV.

background; one at a recoil mass near 2.01 GeV/c^2 and the second near 2.15 GeV/c^2. The most natural interpretation[39] of this recoil mass spectrum is that the 2.01 GeV/c^2 peak corresponds to a state produced in association with the 1.87 GeV/c^2 state, while the 2.15 GeV/c^2 peak represents the kinematic reflection due to pair production of the 2.01 GeV/c^2 object and the subsequent decay of one of these to the 1.87 GeV/c^2 state plus a pion with very small Q-value. Additional data at several values of $E_{c.m.}$ are required to prove this conjecture, however.

To search for charged relatives of the new neutral state near 1.87 GeV/c^2, invariant mass spectra for systems of a charged K and two charged pions have been studied. K$\pi\pi$ combinations with net charge plus or minus one can be divid-

ed into two classes: "nonexotic" combinations where the pions have opposite electric charge (the usual K* channel), and "exotic" combinations where the pions have the same electric charge. In terms of the standard 3-quark model, exotic states cannot be formed from single quark-antiquark combinations. Therefore, the existence of exotic states would provide clues on new particle production.

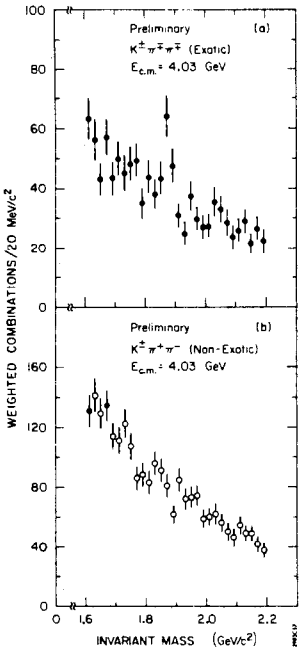

Fig. 21--Invariant mass spectra for time-of-flight weighted combinations of the charged particles Kππ. (a) the exotic combinations $K^{\mp}\pi^{\pm}\pi^{\pm}$, (b) nonexotic combinations $K^{\pm}\pi^{+}\pi^{-}$.

Preliminary invariant mass spectra for Kππ combinations are given in Fig. 21. These data were obtained from the same sample of hadronic events at $E_{c.m.}$ = 4.03 GeV that was discussed above. The Kππ combinations are weighted by their time-of-flight likelihood, but, in this case, the average momenta are sufficiently low to provide much cleaner K-π separation than in the Kπ case. Fig. 21a shows a significant (>5 standard deviations) peak in exotic combinations near 1.87 GeV/c^2, while no corresponding peak is present in nonexotic Kππ combinations. A fit to the exotic mass spectrum gives the mass of the state as 1876 ± 15 MeV/c^2 (systematic errors included) and the full decay width is less than 40 MeV/c^2 at the 90% confidence level. Preliminary values for the cross section times branching ratio for this state are given in Table IV along with values for the neutral state.

The recoil mass spectrum for events within the Kππ peak is shown in Fig. 22. In this case, the background can be estimated accurately by using the nonexotic Kππ combinations in the same invariant mass interval as the exotic signal. As with the Kπ system, we see that this new Kππ state is produced in association with states of comparable or even larger mass. Both recoil mass spectra, Figs. 22 and 20, show a strong peak at a missing mass of 2.01 ± 0.02 GeV/c^2. However, the charged Kππ system does not display the prominent peak near 2.15 GeV/c^2 that is seen in the neutral Kπ recoil mass spectrum. Owing to the very small phase space available for producing these 1.87 GeV/c^2 states in association with 2.15 GeV/c^2 systems, and because the related 2.01 GeV/c^2 recoil mass peaks are so close to being just one pion mass heavier than the 1.87 GeV/c^2 states, electromagnetic mass splittings between the various states will be of crucial importance to the observed rates,[39] and we must again appeal to more experimental work to understand the details of these recoil mass spectra.

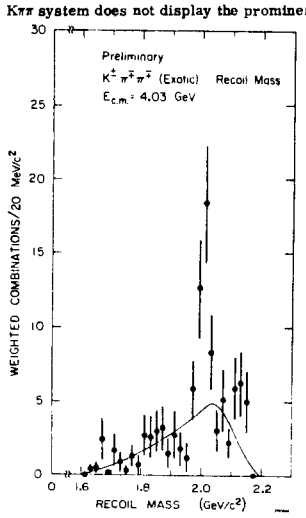

Fig. 22--Recoil mass spectrum for events in the 1.87 GeV/c^2 exotic Kππ peak. The solid curve is the background estimated from nonexotic combinations.

The 4 GeV region in e^+e^- annihilation has provided obvious attraction since it was first known that R doubles over this energy range with several prominent and rather broad structures. Now this region is beginning to yield answers to some of our questions. New states, both neutral and charged, are being produced with thresholds in the 4 GeV region. In particular, a charged state of mass 1876 ± 15 MeV/c^2 and a neutral state of mass 1865 ± 15 MeV/c^2 are by now well established. It is significant that the energies for pair producing these states lie in the small region between the very narrow ψ' and the broader structures near 4 GeV. The yield of the neutral 1.87 GeV/c^2 object is strongly correlated with the structure in R. Both states have narrow decay widths, consistent with the lifetimes expected of weakly decaying objects. In all cases observed to date, the decays of these states involve K mesons and the charged state is seen only in the exotic combinations $K^{\mp}\pi^{\pm}\pi^{\pm}$ and not in the corresponding nonexotic combinations or in combinations with electric charge greater than one. I find the evidence to be persuasive that these states are the predicted[40] isodoublet of charmed mesons, (D^+,D^0). Their preference for decays involving K mesons, particularly the exotic channel, is dramatic evidence for the charm-strangeness relationship proposed by Glashow, Iliopoulos, and Maiani.[41]

TABLE IV

Preliminary cross sections times branching ratios for the new states near 1.87 GeV/c^2 in mass. σ_n is the total hadronic cross section.

Decay Mode	$\sigma \cdot$ BR (nb) for $3.9 \leq E_{c.m.} \leq 4.6$ GeV (σ_n = 27 ± 3 nb)	$\sigma \cdot$ BR (nb) for $E_{c.m.}$ = 4.03 GeV (σ_n = 33 ± 5 nb)
$K^{\pm}\pi^{\mp}$	0.20 ± 0.05	0.52 ± 0.05
$K^{\mp}\pi^{\pm}\pi^{\pm}$	---	0.27 ± 0.05
$K^{\pm}\pi^{\mp}\pi^{+}\pi^{-}$	0.67 ± 0.11	0.72 ± 0.18

Note: Systematic errors on all values are ±50% due to present uncertainty in detection efficiencies.

Questions for the next generation of experiments abound. There is a whole new world of charmed particles to discover and study. We would still like to understand the structure in R. My question to this rapporteur at the next International Conference on High Energy Physics is a simple one: What else is happening in the 4 GeV region?

I want to thank our Soviet colleagues, members of the Organizing Committee, and particularly my scientific secretaries for making my short stay in the Soviet Union such a pleasant one.

REFERENCES

1. B. Richter, Proc. XVII Int. Conf. on High Energy Physics, London, 1-10 Jul 1974 (Rutherford Lab, Chilton, 1974), p. IV-37.
2. E. de Rafael, invited talk, this Conference.
3. S. D. Drell, Ann. Phys. (N.Y.) 4, 75 (1958). T. D. Lee and G. C. Wick, Nucl. Phys. B 9, 209 (1969). N. M. Kroll, Nuovo Cimento A 45, 65 (1966).
4. B. L. Beron et al., contributed paper #1124/B1, this Conference.
5. B. L. Beron et al., Phys. Rev. Lett. 33, 663 (1974).
6. F. A. Berends, K. J. F. Gaemers, and R. Gastmans, Nucl. Phys. B 68, 541 (1974); Nucl. Phys. B 57, 381 (1972); Nucl. Phys. B 75, 546 (197). F. A. Berends and R. Gastmans, Nucl. Phys. B 61, 414 (1973).
7. J.-E. Augustin et al., Phys. Rev. Lett. 34, 233 (1975).
8. J.-E. Augustin et al., Phys. Rev. Lett. 30, 462 (1973).
9. A. M. Boyarski et al., Phys. Rev. Lett. 34, 1357 (1975). V. Lüth et al., Phys. Rev. Lett. 35, 1124 (1975).
10. V. M. Aulchenko et al., Novosibirsk preprint 75-65 (1975); see also Ref. 18.
11. C. Bacci et al., Phys. Lett. B 58, 481 (1975).
12. B. Esposito et al., Phys. Lett. B 58, 478 (1975).
13. R. Baldini-Celio et al., contributed paper #1100/N2, this Conference.
14. A. M. Boyarski et al., Phys. Rev. Lett. 34, 762 (1975).
15. R. F. Schwitters, Proc. 1975 Int. Symposium on Lepton and Photon Interactions at High Energies, Stanford University, 21-27 Aug 1975 (SLAC, Stanford, California, 1975), p. 5.
16. H. L. Lynch, talk presented at Int. Conf. on Production of Particles with New Quantum Numbers, U. Wisconsin, Madison, 22-24 April 1976.
17. Maryland-Princeton-Pavia-San Diego-SLAC Collaboration, paper contributed to this Conference.
18. V. A. Sidorov, invited talk, this conference.
19. S. Jullian, invited talk, this conference.
20. M. Conversi et al., Phys. Lett. B 52, 493 (1974). V. Alles-Borelli et al., Nuovo Cimento A 30, 136 (1975). V. E. Balakin et al., Phys. Lett. B 41, 205 (1972).
21. Review talk by C. Bemporad, Proc. 1975 Int. Symposium on Lepton and Photon Interaction at High Energies, Stanford University, 21-27 Aug 1975 (SLAC, Stanford, California, 1975), p. 113.

22. G. J. Gounaris and J. J. Sakurai, Phys. Rev. Lett. 21, 244 (1968).
23. A. N. Skrinsky, invited talk, this Conference.
24. G. Hanson, invited talk, this Conference. (SLAC-PUB-1814)
25. J.-E. Augustin et al., Phys. Rev. Lett. 34, 7[illegible] (1975).
26. H. Harari, Proc. 1975 Int. Symposium on Lepton and Photon Interactions at High Energies, Stanford University, 21-27 Aug 1975 (SLAC, Stanford, California, 1975), p. 317.
27. R. F. Schwitters and K. Strauch, Ann. Rev. Nucl. Sci. 26, 89 (1976).
28. J. Whitmore, Phys. Rep. C 10, 273 (1974).
29. Ya. I. Azimov, L. L. Frankfurt, and V. A. Khoze, contributed paper #1183/N2, this Conference.
30. Y. S. Tsai, Phys. Rev. D 12, 3633 (1976).
31. R. P. Feynman, Photon-Hadron Interactions (W. A. Benjamin, New York, 1972).
32. G. Hanson et al., Phys. Rev. Lett. 35, 1609 (1975).
33. R. F. Schwitters et al., Phys. Rev. Lett. 35, 1320 (1975).
34. J. Siegrist et al., Phys. Rev. Lett. 36, 700 (1976).
35. J. Kogut and L. Susskind, Phys. Rev. D 12, 2821 (1975). E. Eichten et al., Phys. Rev. Lett. 35, 500 (1976). K. Lane and E. Eichten, Phys. Rev. Lett. 37, 477 (1976).
36. L. B. Okun, private communication. M. Bander et al., Phys. Rev. Lett. 36, 695 (1976). C. Rosenzweig, Phys. Rev. Lett. 36, 697 (1976).
37. G. Goldhaber et al., Phys. Rev. Lett. 37, 255 (1976).
38. Present members of the SLAC/LBL collaboration are: G. S. Abrams, M. S. Alam, A. M. Boyarski, M. Breidenbach, W. C. Carithers, W. Chinowsky, S. C. Cooper, R. G. DeVoe, J. M. Dorfan, G. J. Feldman, C. E. Friedberg, D. Fryberger, G. Goldhaber, G. Hanson, J. Jaros, A. D. Johnson, J. A. Kadyk, R. R. Larsen, D. Lüke, V. Lüth, H. L. Lynch, R. J. Madaras, C. C. Morehouse, H. K. Nguyen, J. M. Paterson, M. L. Perl, I. Peruzzi, M. Piccolo, F. M. Pierre, T. P. Pun, P. Rapidis, B. Richter, B. Sadoulet, R. H. Schindler, J. Siegrist, W. Tanenbaum, G. H. Trilling, F. Vannucci, J. S. Whitaker, J. E. Wiss.
39. A. De Rújula, Howard Georgi, and S. L. Glashow, Phys. Rev. Lett. 37, 398 (1976).
40. J. D. Bjorken and S. L. Glashow, Phys. Rev. Lett. 11, 255 (1964); M. K. Gaillard, B. W. Lee, and J. L. Rosner, Rev. Mod. Phys. 47, 277 (1975).
41. S. L. Glashow, J. Iliopoulos, and L. Maiani, Phys. Rev. D 2, 1285 (1970).

*Work supported by the Energy Research and Development Administration. (Rapporteur talk presented at the XVIII International Conference on High Energy Physics, Tbilisi, USSR, 15-21 July 1976.)

HADRONS PRODUCED IN DEEP INELASTIC MUON SCATTERING AT HIGH ENERGIES*

A.L.Sessoms

Harvard University

I will present data taken by the Chicago-Harvard-Illinois-Oxford (CHIO) collaboration at Fermilab and a result on shadowing by a group from the Moscow Physical Engineering Institute. CHIO[1-4].

The process we will discuss is shown in Fig.1.

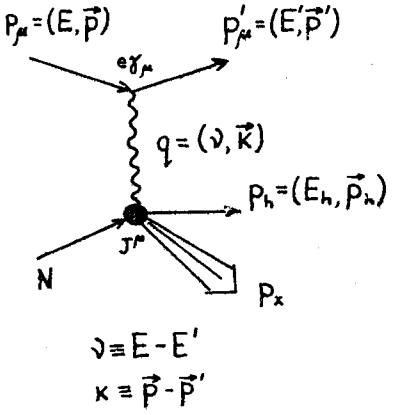

Fig. 1

A muon of known momentum is scattered, suffering an energy loss, ν , and transfering a virtual photon of momentum q to a nucleon N . The scattered muon and hadron resulting from the virtual photon-nucleon interaction are detected in the apparatus shown in figure 2. The target

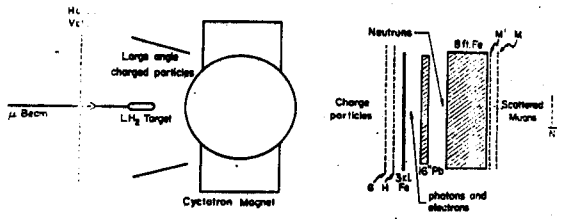

Fig. 2

was liquid hydrogen or liquid deuterium. The incident muon energy was 150 GeV. The scattered muon was identified by its ability to transverse approximately $2\frac{1}{2}$ meters of iron.